Fatigue Assessment of a Rear Axle for Light Trucks

Stefano Beretta [a], Michele Carboni [a], Hernàn Desimone [b], Edgardo Lòpez [b]

[a] Politecnico di Milano, Milano, Italy
[b] Tenaris/Dalmine, Dalmine, Italy

Abstract In the present paper, the fatigue assessment of welded components, in particular the axle beam of a rear axle for light trucks, is presented. The analysis starts with in-service measurements of actual loads. In order to obtain these data, load spectra measurements were performed on urban, extra-urban, high-way and off-road conditions. Then, by means of finite element analyses, the stresses in the component were obtained and post-processed by means of two different techniques for the assessment of welding joints: "Hot Spot" method and Local Stress. The results were eventually discussed and validated through full scale testing. Considering the possible presence of inhomogeneities, a fitness-for-purpose analysis has also been carried out and compared with experimental full-scale tests on axles beams.

1 INTRODUCTION

Welded components require careful design and realization due to the fact that welds can be their most critical points. Different methods are available in literature for life prediction and design of welds, among them it is possible to recall: Hot Spot [1,2], Local Stress [3,4] and Fracture Mechanics [3,4]. The critical situation is even more delicate considering those components subjected to fatigue loads, such as in the automotive field, because the application of the predicting methods is based on the availability of reliable and well-describing service loads and on fatigue strength curves possibly obtained by full-scale tests.

In the first part of the present paper, we will address the fatigue assessment of welded components, in particular the axle beam of a rear axle for light trucks. The analysis started with in-service measurements of actual loads. In particular, load spectra measurements were performed on urban, extra-urban, high-way and off-road conditions. The load spectra will be used in order to derive an equivalent constant amplitude load to be applied at the bench during full-scale tests of the components. Then, by means of finite element analyses, the stresses in the component will be obtained and post-processed by means of two different techniques for the assessment of welded joints: "Hot Spot" and "Local Stress" methods. The results will be finally compared with full-scale tests.

In the second part, we will consider the possible presence of inhomogeneities onto the rear axle body due to the application of acceptability criteria or to the probability of detection during Ultrasonic Non Destructive Testing. To this aim, a fitness-for-purpose analysis [5] has been carried out based onto fracture mechanics experiments and the application of a crack propagation algorithm. Prediction were then validated by full-scale tests carried out on rear axles containing suitable artificial defects.

2 MEASUREMENT OF SERVICE LOADS

In order to define a load history to be applied at the bench during the full-scale tests of the rear axle beam (in the following simply named "rear axles"), a light truck (Figure 1a) was tested in service with the aim of measuring the typical load spectra of rear axles. In particular, the considered rear axle (Figure 1b) is built in 20MnV5 steel and is formed by two tubes press-fitted into a carrier box. Moreover, two supports for dampers and two brackets for leaf springs are welded on the tubes.

Horizontal and vertical bending stresses (in the last case on both sides of the carrier box) were derived from strain gages measurements (Figure 2a). The total load carried by the truck during the tests was formed by the wooden box and the payload (steel tubes) shown in Figure 2b. It is worth noting that this payload corresponds to 70% of the maximum payload transportable by the considered truck. All the measurements were classified, grouped and elaborated into stress time histories according to four different road types: highway, urban, extra-urban and off-road. Figures 2c and d show some examples of extra-urban and off-road routes.

(a) (b)

Figure 1. Measurements of service loads: a) the considered truck; b) rear axles and carrier box.

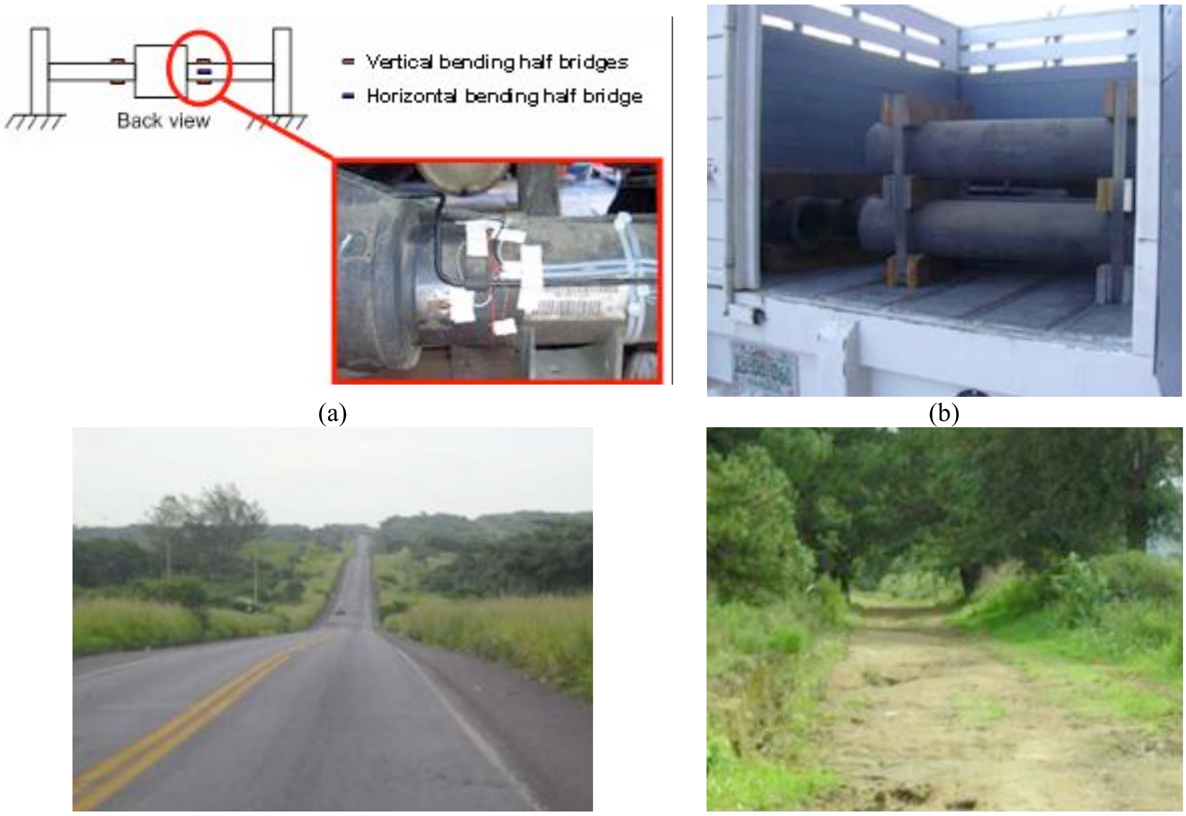

(a) (b)

(c) (d)

Figure 2. Test set-up: a) schematic of the instrumentation mounted on the rear axle; b) carried payload; c) and d) examples of extra-urban and off-road routes, respectively.

2.1 Post-elaborations applied to the experimentally derived load histories

As said in the previous paragraph, the measurements were carried out with the light truck loaded at 70% of the maximum transportable payload. In order to carry out experimental full-scale tests considering the worst case, it was then necessary to derive the load spectra to keep into account for the application of the 100% maximum transportable payload. This was achieved assuming a linear behaviour of the service loads with payload and so they were amplified by a suitable multiplication factor. The obtained stress time histories were transformed, by means of geometry considerations, in terms of load time histories eventually elaborated in order to filter them from those low amplitude cycles that are below a given threshold and not significantly damaging.

Eventually, the filtered load time histories were statistically extrapolated in order to consider longer service times in respect to the measured ones. This was achieved by means of the Statistics of Extremes Values [6] and, in particular, applying a novel extrapolation method [7] based on the Peak Over Threshold technique [8]. Table I shows the comparison between the measured distances for each type of route and the ones extrapolated twelve times, while Figure 3a shows the example of the highway route in the case of the left vertical bending. In the present study, the left vertical bending will be the only considered case since it produced, during the measurements, the highest loads on the rear axle.

Table I – Measured distances and extrapolated ones for each road condition.

Type	Highway	Urban	Extra-urban	Off-road	Total
Measured distances (km)	250	264	525	146	1185
Extrapolated distances (km)	3000	3168	6300	1752	14220

Finally, two more elaborations were applied to load time histories. The first one regards a discretisation of the load spectrum in blocks (Fig. 3b) arranged following a Gassner sequence [9]. This is due to the fact that random sequences of load values are typically very difficult to apply at the test bench. The second elaboration regards, instead, the introduction of the operations of loading and unloading the payload during service (Fig. 3c). The introduction was realized dividing each time history relative to a type of route into smaller parts at whose ends the loading and unloading operations were inserted. A total time history of the measurements has then been derived appending the elaborated signals coming from any route.

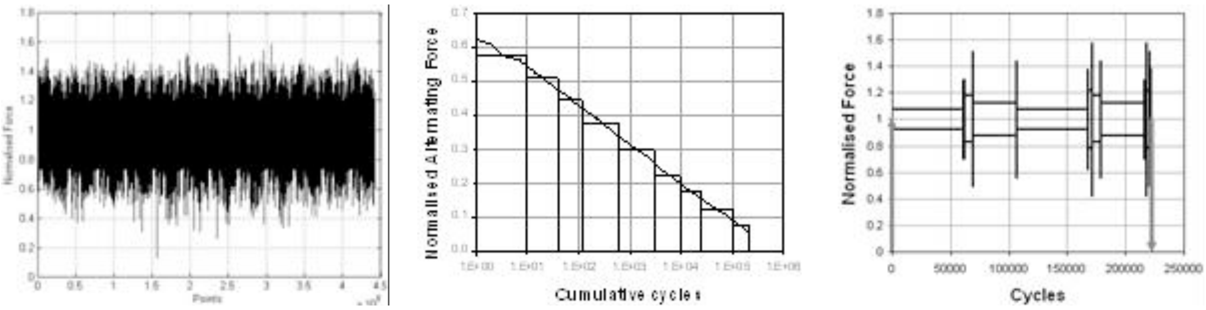

(a) (b) (c)

Figure 3. Vertical bending (left side) for the case of highway route: a) extrapolated and filtered time history (normalised in respect to the mean value); b) block loads representing the load history; c) Gassner sequence of block loads.

3 FATIGUE ASSESSMENT OF REAR AXLE WELDS

Full-scale experimental tests have been firstly carried out discovering the welds to be a critical point for fatigue life of rear axles. The experimental evidences have then been used to validate both the calculations by FEM and the results obtained by Hot Spot and Local Stress methods.

3.1 Full-scale tests on rear axles

Full-scale tests were conducted according to a product validation program based on the calculation of the damage corresponding to the load spectrum measured during service. The program consists in two different constant amplitude fatigue tests representing the actions of vertical bending and cornering, respectively (Figures 4a and b). In order to carry out the tests, different full-scale specimens were mounted on dedicated servo-hydraulic rigs (Figures 4c and d) able to reproduce the two test conditions.

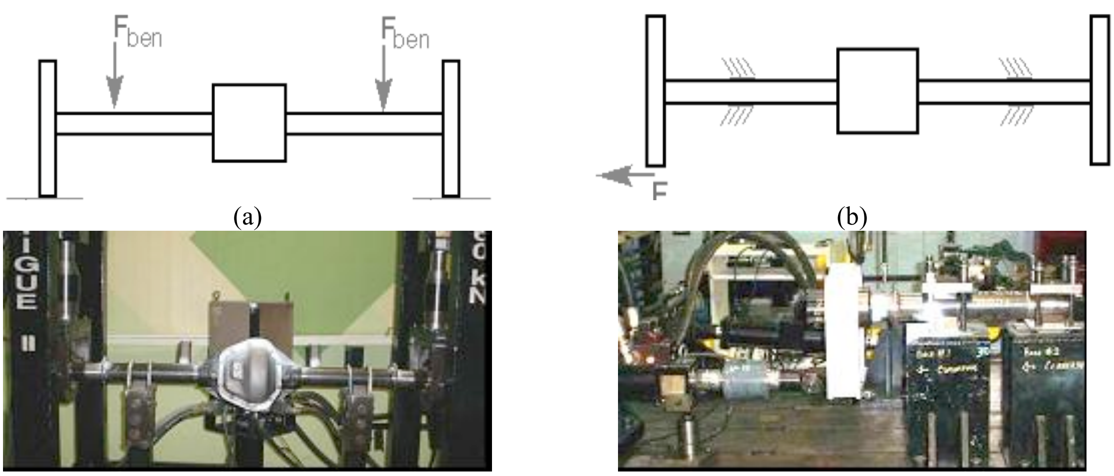

Figure 4. Product validation program: a) schematic of vertical bending test; b) schematics of cornering test; c) and d) test benches for vertical bending and cornering tests, respectively.

The vertical bending test was carried out on 13 specimens in terms of a sinusoidal wave characterized by R=0 and frequency equal to 4 Hz considering an applied $F_{ben,max}$ determined considering the equality between the damages corresponding to the total time history measured during service and the one of the constant amplitude load applied during the tests. Two different kinds of failures could be observed on broken specimens: i) fractures on the rear axle in the zone press-fitted into the carrier box; ii) fractures on the rear axle at the welds of the damper support (Fig. 5a). The cornering test was carried out on 10 specimens in terms of a sinusoidal wave characterized by R=-1 and frequency equal to 3 Hz considering. Mostly one kind of failure could be observed on broken specimens: fractures on the rear axle at the welds of the leaf springs brackets (Fig. 5b).

Some more rear axles were also tested in vertical bending applying block loads. It was then possible to determine a Relative Miner Index equal to about 12 in respect to the fatigue strength curve derived by the Local Stress method and that will be presented in § 3.4 and Fig. 7a.

It can be concluded that the welds are the most critical point for rear axles and so their fatigue behaviour was analyzed by means of finite element analyses.

(a) (b)

Figure 5. Typical failures observed during full-scale tests of rear axles: a) damper support (vertical bending tests); b) leaf spring bracket (cornering).

3.2 FEM analysis of rear axle welds

FEM analyses were then carried out in order to determine the most damaging stresses in the component to be compared with fatigue strength curves. FEM analyses were carried out by means of ABAQUS® software v.6.3 [10]. The rear axle was modelled taking advantage of symmetry and by means of brick elements with 20 nodes. The material was modelled as linear elastic. The applied loads were equal to the F_{ben} and F_{cor} values. Results will be reported as nodal averages extrapolated from the integration points. FEM results are shown in Figure 6. As it can be seen, the most critical points for the stresses are the fillet welds of the damper support and the leaf spring bracket: these points correspond exactly to the failure points observed during full-scale tests (compare with Figure 5).

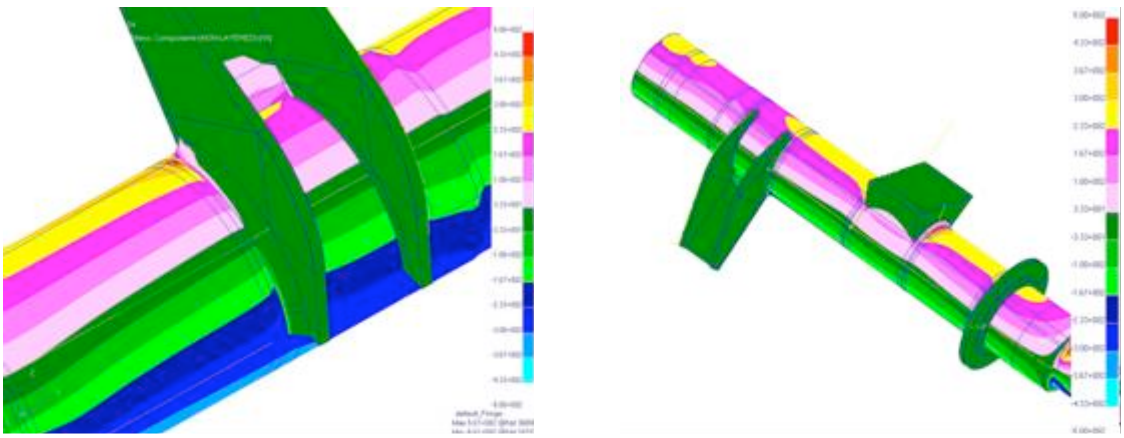

(a) (b)

Figure 6. FEM results for the rear axle: a) detail of the fillet weld of the damper support (vertical bending); b) detail of the fillet weld of the leaf spring bracket (cornering).

3.3 Fatigue assessment by "Hot Spot" method

Considering the stresses shown in Figure 6 for the case of vertical bending, the calculated Hot Spot Stress $\Delta\sigma_{HS}$ [1,2] was equal to 448 MPa. In order to carry out the fatigue assessment, this stress value was compared with the fatigue strength curve suggested by the International Institute for Welding for fillet welds [2]. The resulting number of cycles at failure was equal to approx. 20.000. This result is too conservative (more than one order of magnitude) in comparison with the 50% life of full-scale specimens (Fig. 7a), so suggesting that in the case of rear axles, the Hot Spot method yields too underestimated life predictions. The same conservatorism could be observed in the case of the cornering (Fig. 7b). In order to improve the life prediction of rear axles, the Local Stress method has been applied.

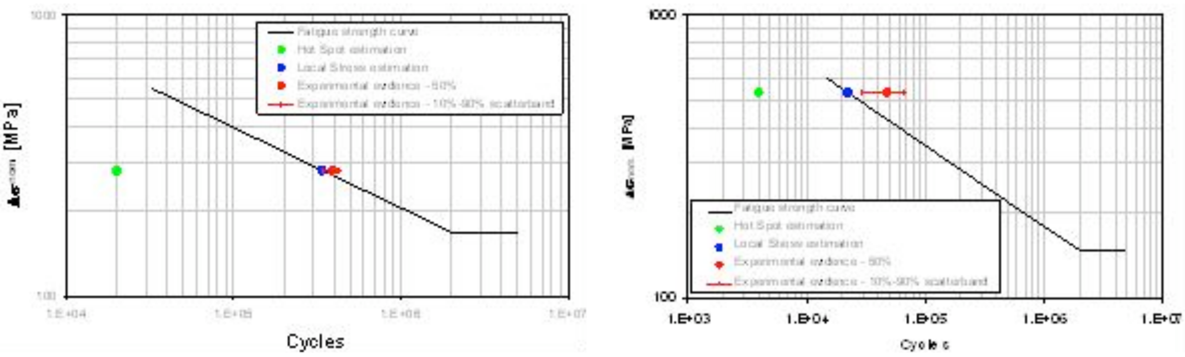

(a) (b)

Figure 7. Comparison between life prediction methods and full-scale experimental evidences: a) vertical bending; b) cornering.

3.4 Fatigue assessment by "Local Stress" method

The "Local Stress" method [3,4] is based on the concept that the weld maximizes the "fatigue notch factor" K_f. The K_f values were then derived, for the vertical and cornering cases, from: i) the FEM results shown in Figure 8a and b that permitted to derive the K_t values; ii) the assumption, for the steel used in the considered rear axle production having UTS=800 MPa, of a notch sensitivity value equal to 0.12. The K_f value was derived by means of the following expression:

$$K_f = 1 + \frac{K_t - 1}{1 + \frac{a^*}{\rho}} \tag{1}$$

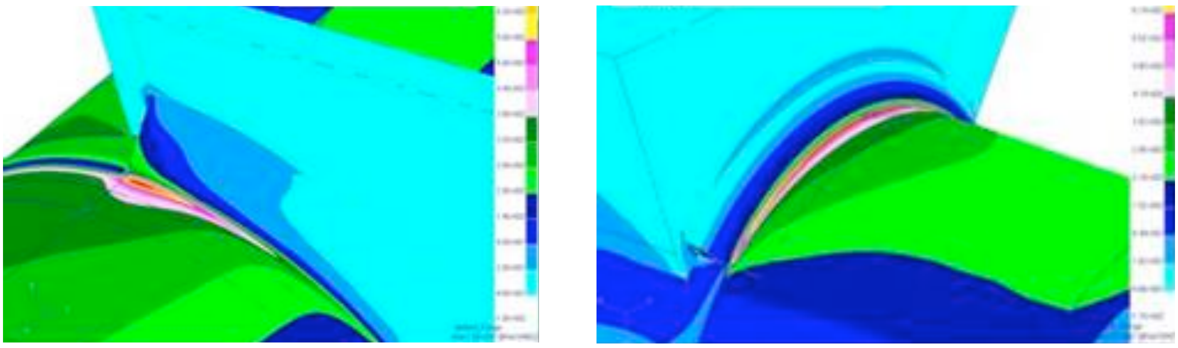

(a) (b)

Figure 8. Local Stress method: a) FEM calculation of K_t for vertical bending; b) FEM calculation of K_t for cornering.

Eventually, the K_f coefficient are used to define the fatigue limit values for the fatigue strength curves (together with the assumption of a slope for the finite life region equal to 3.5). Fatigue assessment could then be carried out by means of the nominal stress acting on the rear axle and the fatigue strength curves (Figure 7). In the case of vertical bending, the found number of cycles at failure was equal to approx. 340.000, a value very close to the 10% percentile of life observed during full-scale tests (Figure 7a). In the case of cornering, the same conclusions could be drawn (Figure 7b). It can be concluded that the Local Stress method is able to produce effective life predictions suitable for design and design improvements of rear axles.

4 FITNESS-FOR-PURPOSE OF REAR AXLE BEAMS

All the produced rear axles are controlled by means of Ultrasonic Non Destructive Testing before being released to the market. The threshold defect dimension for accepting or rejecting a given rear tube is agreed with customers and depends on the stress level. In order to check the behaviour of an accepted rear axle containing defects in the body, in the present part of the paper fracture mechanics experiments have been carried out and a propagation model applied. Predictive results have then been compared with dedicated full-scale experiments.

Fracture mechanics experiments have been carried out adopting SE(B) specimens (Fig. 9a) obtained directly from tubes in 20MnV5 steel. Crack length has been measured adopting a potential drop technique realised by means of crack-gages (Fig. 9b) and a FRACTOMAT® control unit. Tests were carried out to derive both the linear and the threshold regions of the crack propagation curves at R=-1, 0.05, 0.1 and 0.3 following the suggestions by ASTM E-647 [11]. Figure 9c shows all the obtained crack propagation curves normalised in respect to the threshold SIF range derived at R=0.05.

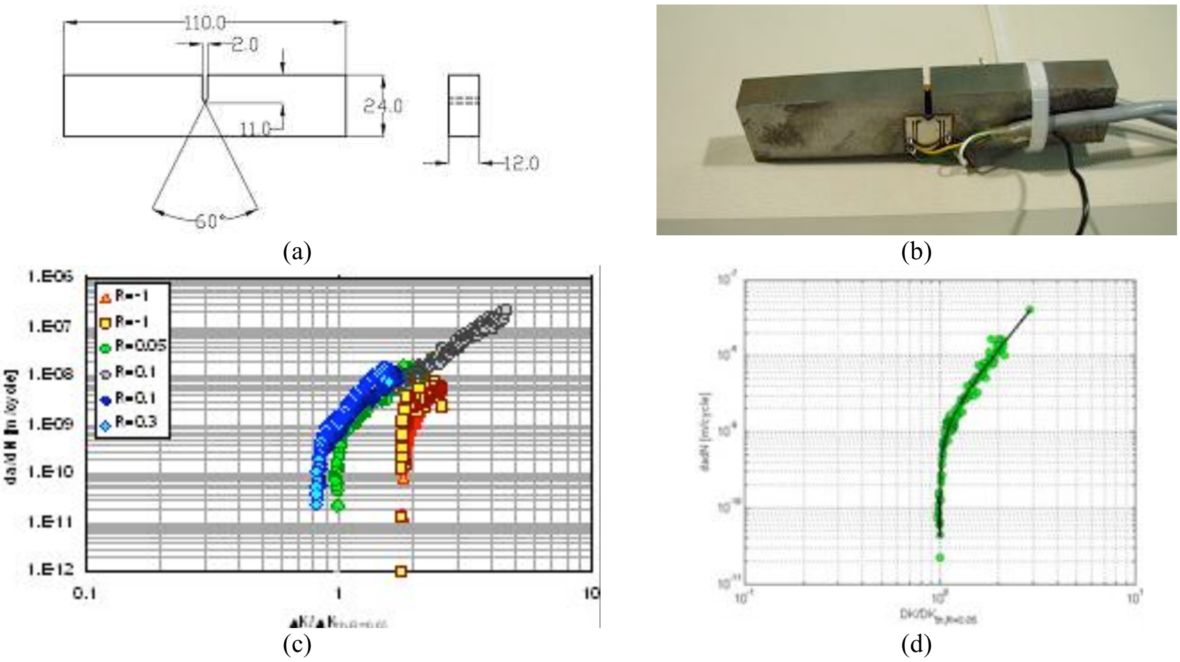

Figure 9. Fracture mechanics experiments: a) SE(B) specimen; b) application of crack gages; c) crack propagation curves for 20MnV5 steel (normalised on $\Delta K_{th,R0.05}$); d) crack growth data fitting at R=0.05.

Crack growth data could then be interpolated (Fig. 9d) by means of the so-called "NASRO Equations" [12]:

$$\frac{da}{dN} = C\left[\left(\frac{1-f}{1-R}\right)\Delta K\right]^n \frac{\left(1-\frac{\Delta K_{th}}{\Delta K}\right)^p}{\left(1-\frac{K_{max}}{K_{crit}}\right)^q} \tag{2}$$

$$\Delta K_{th} = \Delta K_0 \left(\frac{a}{a+a_0}\right)^{\frac{1}{2}} / \left(\frac{1-f}{(1-A_0)(1-R)}\right)^{(1+C_{th}R)} \tag{3}$$

In particular, Eq. (2) describes the da/dN-ΔK relationship for all the propagation regimes (threshold, Paris and instable growth) and its parameters are: C, n, p and q are empirical constants, ΔK_{th} is the threshold SIF range, K_{max} is the maximum applied SIF and K_{crit} the critical SIF. The most important parameter is f, representing the crack closure effect [13]. This parameter depends on the constraint factor α, on the ratio between the maximum applied stress and the yield stress and on the stress ratio.

Eq. (3), instead, describes the ΔK_{th}-R relationship and its parameters are: f is again the closure function, A_o is a constant defined in f, ΔK_o is the threshold SIF range at R=0, C_{th} is an empirical constant and a_0 is the El-Haddad's parameter. The dependence of ΔK_{th} on stress ratio is controlled by the parameter C_{th}: different values of C_{th} (namely C_{th+} and C_{th-}) have to be considered for positive and negative R values. It should be noted that Eq. (3) is in general valid in the range $-2 \leq R \leq 0.7$: outside this range, threshold data tend to be constant.

Eventually, the calibrated model has been systematically applied in order to estimate the propagation lifetime of rear axles containing surface defect depths from 0.1 mm to 0.4 mm (Fig. 10a).

In order to validate the propagation lifetime estimates, a full-scale test was carried out. In particular, an artificial defect characterised by dimensions equal to 5 length x 0.3 width x 0.4 depth mm (this depth corresponds to 4% tube thickness) has been introduced onto a rear axle (Fig. 10b) eventually tested in vertical bending conditions at constant amplitude load. Figure 10a shows the comparison between predictions and the experimental result: an error equal to 5.4% could be determined. It must be added that more validation tests have been carried out successfully on small-scale specimens containing artificial defects and subjected to block loads.

It can be concluded that the calculation method adopted here permits to effectively manage those cases where a defect is present onto the body of the rear axle. A further interesting application can be the tuning of a suitable and optimised NDT threshold based onto the desired lifetime.

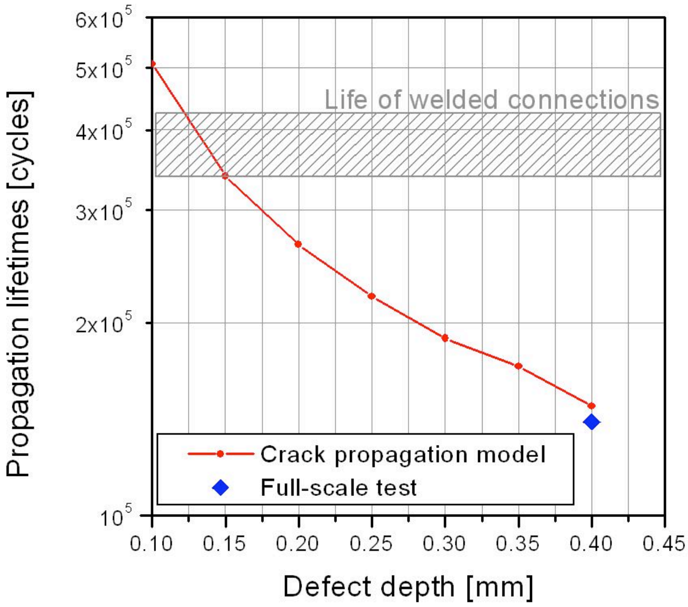

(a)

(b)

Figure 10. Estimated propagation lifetimes (a) and experimental full-scale bending fatigue test considering a 5 L x 0.3 w x 0.4 d mm artificial defect (b).

5 CONCLUDING REMARKS

In the present paper, the fatigue assessment of welded components, in particular the axle beam of a rear axle for light trucks, has been addressed. The analysis started with in-service measurements of actual loads. In particular, load spectra measurements were performed on urban, extra-urban, high-way and off-road conditions. The load spectra were used in order to derive an equivalent constant amplitude load to be applied at the bench during full-scale tests of the components. Then, by means of finite element analyses, the stresses in the component were obtained and it was found a very good correspondence between the maximum numerical stress values and the fracture locations on full-scale specimens. FEM results were then post-processed by means of two different techniques for the assessment of welded joints: "Hot Spot" and "Local Stress" methods. The results showed that the Hot Spot method, for the case of rear axles, produces too conservative predictions, while Local Stress method is able to well describe fatigue life of rear axles. Finally, the fitness-for-purpose analysis of the body of rear axles containing defects has permitted to set up a crack propagation algorithm able to produce life estimates very close to experimental full-scale results. This method can be successfully applied to manage "worst cases" and to tune NDT inspections.

6 ACKNOWLEDGEMENTS

The present research activity has been carried out in a Research Contract between Politecnico di Milano and Tenaris/Dalmine. The authors would like to thank Dr. Mario A. Rossi, Director of Tenaris/Dalmine R&D, for supporting the research.

7 REFERENCES

1. E. Niemi, Stress Determination for Fatigue Analysis of Welded Components, IIW-Doc. IIS/IIW-1221-93, International Institute of Welding, 1995.
2. S.J. Maddox, Hot-Spot Stress Design Curves for Fatigue Assessment of Welded Structures, IIW-Doc. XIII-1900a-00, International Institute of Welding, 2000.
3. D. Radaj, Design and Analysis of Fatigue Resistant Welded Structures, Woodhead Publishing Ltd, 1990.
4. D. Radaj, C.M. Sonsino, Fatigue Assessment of Welded Joints by Local Approaches, Woodhead Publishing Ltd, 1998.
5. European Fitness-for-service Network, FITNET FFS Procedure, Final Draft MK7, 2006.
6. E.J. Gumbel, Statistics of Extremes, Columbia University Press, 1957.
7. P. Johannesson, *Fatigue Fract. Engng Mater. Struct.*, 29, 2006, 201-207.
8. R.D. Reiss, M. Thomas, Statistical Analysis of Extreme Values, Birkhauser Verlag, 1997.
9. V. Grubisic, Criteria and methodology for lightweight design of vehicle components, Technical Report #TB-176. LBF, Darmstadt, 1986.
10. ABAQUS v.6.3, User Manual, 2004.
11. ASTM E647-00, Standard test method for measurement of fatigue crack growth rates, Philadelphia: ASTM, 1994.
12. Anonymous. Fatigue crack growth computer program "NASGRO" version 3.0 – reference manual. Technical Report JSC-22267B, NASA, 2001.
13. Elber W. The significance of fatigue crack closure. In: Damage tolerance in aircraft structure, ASTM STP.1971;486:230-242.